Progress in Organic Coatings 175 (2023) 107373

Contents lists available at ScienceDirect

Progress in Organic Coatings

journal homepage: www.elsevier.com/locate/porgcoat

Key parameters and mechanism of blistering of coil-coatings in humid-hot laboratory environments

Barbara Obereigner [a,b,*], Georg Mayr [b], Bernhard Strauß [b], Peter Bognar [c], Sonny Ngo [d], Klaus Bretterbauer [a], Christian Paulik [a]

[a] Institute for Chemical Technology of Organic Materials, Linz Johannes Kepler University, Altenberger Straße 69, 4040 Linz, Austria
[b] voestalpine Stahl GmbH, voestalpine-Straße 3, 4020 Linz, Austria
[c] Becker Industrial coatings, Norfer Str. 3, 41539 Dormagen, Germany
[d] Becker Industrial coatings Long term development group (LTD), Goodlass Rd, L24 9HJ Liverpool, United Kingdom

ARTICLE INFO

Keywords:
Osmotic blistering
Coil coatings
Leaching
Anticorrosive pigments
Accelerated laboratory testing
Organic coatings

ABSTRACT

Blistering of organic coatings on hot dip galvanized (HDG) steel is of high practical relevance, especially in warm-humid environments. The aim of this work was to study the key parameters of blister formation and growth by accelerated laboratory testing at 60 and 70 °C. Following a statistical design of Taguchi, the components of a polyurethane (PU) primer formulation were varied and applied to hot-deep galvanized (HDG) steel. The presence of a topcoat was found to be a precondition for blistering. Degradation started at microcracks within the primer and was significantly influenced by the adhesion between primer and topcoat. A high content of anticorrosive pigments resulted in enhanced blister formation, while blister growth is mainly controlled by mass transport processes and shows a strong temperature dependence. This study focuses on one specific blistering mechanism, osmotic blistering, which is indicated by blister kinetics and leachate analysis, estimated pressure values inside the blister are in reasonable agreement by using two different calculation approaches.

1. Introduction

Blistering of organic coatings is a widespread phenomenon in material degradation and understanding the causes has achieved considerable attention over the years due to its practical relevance in enhancing the lifetime of polymeric materials, linings, and coated products – especially organic coated metals.

Evaluation of coating resistance against blistering under humid hot conditions is a widely used technological testing method in coating development covered by numerous standards [ISO 6271, ISO 2812, ASTM D 2247, ASTM D 4585] and is an integral part of many coating specifications. Testing techniques [1–4] usually differ in testing temperature and time, angle of exposure as well as access of the testing medium to the coated panels (one- or double-sided). Common features for these types of tests are that a film of condensed, pure water covers the coating surface and after a certain time of exposure often results in the formation of blisters.

The Q-Panel condensation test (QCT40) (ATM D4585, ISO 6270) is one of the most frequently used accelerated weathering tests. Samples are exposed to water vapor, which condenses at the coated surface, where an additional thermal gradient due to direct contact of the backside with ambient (i.e., cooler) air is induced. In contrast to the accelerated condensation test in this work, the QCT40 test is performed at a lower temperature (40 °C) and a lower tilting angle (15°). Another common approach to test the blister sensitivity of coated products is time-dependent water exposure at elevated temperatures in a simple immersion test using a Bac-Ford bath (EN 13523–9, ISO 2812-2).

Several basic mechanisms of blister formation in organic coatings are known for many years, amongst them osmotic blistering [5,6], cathodic blistering [7] and cold wall blistering [8] to name just the most prominent ones. One superior aspect in relation to blister initiation and growth on organic coated metals is, that blistering is transport-controlled and governed by various types of gradients (water distribution, thermal, ionic, electrical).

Osmotic blistering is the most common mechanism [5,9–11] where the organic coating acts as a semipermeable membrane and the blisters grow due to a concentration gradient between the inside and the outside of the osmotic cell. Several single aspects of osmotically driven blister

* Corresponding author at: Kleinmünchen, 4030 Linz, Austria.
E-mail address: barbara.obereigner@gmail.com (B. Obereigner).

https://doi.org/10.1016/j.porgcoat.2022.107373
Received 21 September 2022; Received in revised form 9 December 2022; Accepted 12 December 2022

formation have been studied in the past [5,9,12–14].

Van der Meer-Lerk [5,13] investigated the influence of concentrations of soluble salts on the metal surface and found a proportional correlation of blister growth and the number of species present at the interface between metal and paint. Twenty years later, Sinko [10] showed that the leaching velocity of chromates used as inhibiting pigments correlated with blistering and delamination kinetics of the coating. Recent works focuses on the leaching mechanisms of connected clusters of corrosion inhibiting pigments [10,15,16] and the slow dissolution of filler particles, more specifically of barium sulfate in chromate solutions and formation of the less soluble barium chromate [17].

Cathodic blistering occurs in proximity of a defect at the metal (M, e.g., Fe or Zn) which is oxidized from M to M^{2+} and O_2 present in water is reduced to OH^-. A high alkaline environment causes a loss of adhesion, leading to delamination and blistering. [18,19] A further important blistering mechanism is cold-wall blistering. The prerequisite for cold-wall blistering is a temperature gradient between a hot, exposed side and a cold, unexposed side of the coating. Water transport occurs from the hot, exposed side to the colder interface, and blisters develop. [8]

However, under real world conditions blistering occurs as a coincidence of several critical factors e.g., a critical time-temperature-humidity regime plus local or systematic weaknesses in the coating layer, maybe additionally intensified by exterior ionic contamination and corrosive degradation (“multi-directional game”) [20–22]. Thus, the interaction of the components of a coating system with water under cold wall conditions is a topic worth to be studied in more detail in order to contribute to a better understanding of the complex phenomenon “blistering”.

In this work, we build on the knowledge summarized above and try to work out a more holistic picture by studying the blister formation kinetics of a broad matrix of experimental primer formulations with and without topcoat in a condensation type blister test (QCT) at different temperatures. The key parameters identified by statistical evaluation are discussed by applying complementary analytical techniques to prove the dominant mechanisms of blister formation.

2. Experimental

2.1. Materials and sample preparation

2.1.1. Coatings to study the cold wall effect

The cold-wall effect (i.e., the temperature difference between exterior and interior surface temperature during condensation) was studied on a commercial coil-coating. HDG steel with a zinc layer (138 g/m^2 at each side) and a sheet thickness of 0.47 mm was alkaline degreased and pretreated (chromium-free Granodine MNT 1455® from Henkel AG & Co.). A commercially available primer based on a polyurethane (PU) resin was topcoated with a polyamide (PA)-structured PU topcoat (T_g of 35 °C), each with a dry film thickness (DFT) of 25 µm.

2.1.2. Model coated samples based on Taguchi Design of Experiments (DoE)

The model primer coatings were based on a polyester-polyol resin. The formulation concept was based on a Taguchi-Design of Experiment proposed by Becker Industrial Coatings and configured in Excel (Microsoft Corporation). (Details see Appendix A). Four parameters were defined (a = anticorrosive pigment content, b = OH/NCO ratio, c = Trimer type and d = blocking agent) in two levels (high and low level) as summarized in Table 1. The isocyanate crosslinkers varied were isophorone diisocyanate (IPDI) and hexamethylene diisocyanate (HDI). Also, the blocking agents ε-caprolactam (Capro) and 3,5-dimethylpyrazole (DMP) were compared. The matrix was applied to two different anticorrosive pigments, a calcium (18 %) ion-exchanged amorphous silica with the trade name Shieldex C303 (W. R. Grace & Co.) and an aluminum triphosphate (ATP) with 28 % MgO, which is commercially available as K-White G-105 (Tayca Corporation). In total, 16 Primers were obtained which were abbreviated with P1-P16 (Table 2).

Table 1
Model primer components as input parameters for a Taguchi DoE design. Shieldex C303 and K-White G-105 were used as anticorrosive pigments.

Entry		High level (HL)	Low level (LL)
1	Anticorrosive pigment (a)	8.6 %	4.3 %
2	OH/NCO ratio (b)	1/1.5	1/1.2
3	Isocyanate trimer (c)	HDI	IPDI
4	Blocking agent (d)	Capro	DMP

A Zn-Al-Mg coated steel (approx. 2 % Al and 2 % Mg, 60 g/m^2 at each side) with a sheet thickness of 0.45 mm (voestalpine Stahl GmbH) was used as a substrate for the organic coatings.

Substrates were degreased by using an alkaline solution at pH 10 and 40 °C. Thereafter, the steel sheets were pretreated by immersion for 5 s in Granodine MNT 1455 (Henkel AG & Co.) at 35 °C and dried at 70 °C. The model primers were applied with by wire bars (RD Specialties, Inc.) and cured for 19 s in an air-circulating oven (Hofmann Wärmetechnik GmbH) at 300 °C to reach a peak metal temperature (PMT, i.e., temperature required to achieve fully crosslinking) of 228 °C. All primer coatings had a DFT of 6 µm. Subsequent a commercial grey coil-coating polyvinylidene difluoride and acrylate (70/30) (PVDF) with a PMT of 254 °C was applied as a topcoat to all primers. The DFT of this topcoat was 20 µm.

2.1.3. DoE evaluation

The degree of blistering after 14 days exposure to the condensation test was assessed visually and evaluated with a simple calculation method by using Taguchi design format.

2.1.3.1. Low level (LL) and high level (HL). The parameters a-d were employed in two levels, a low level (LL) and a high level (HL) according to Table 1. The significance of each parameter was investigated by calculating the difference between HL and LL by subtracting the mean value of the LL blistering results from the mean value of the HL blistering results. A difference of >0.99 is considered as significant, a value between 0.5 and 0.99 as a difference and < 0.49 as no difference. If the difference is positive, it is a HL influence and if it is negative values, it is a LL influence respectively.

2.1.3.2. Interactions between the parameters. The interactions of the parameters a-d in two levels (1 = high level and 2 = low level) were

Table 2
Model primer components. The PU primer coatings (P1-P16) were applied with a wire bar (dry film thickness of 6 µm) to HDG steel and topcoated with the polyvinylidene difluoride (PVDF) and acrylate (70/30) (denoted as topcoat 1 (TC1), dry film thickness of 20 µm).

Primer (P)	Pigment	Pigment content (a)	OH/NCO ratio (b)	Trimer (c)	Blocking agent (d)
P1	Shieldex	8,6 %	1:1.5	HDI	Capro
P2	Shieldex	8,6 %	1:1.5	IPDI	DMP
P3	Shieldex	8,6 %	1:1.2	HDI	DMP
P4	Shieldex	8,6 %	1:1.2	IPDI	Capro
P5	Shieldex	4,3 %	1:1.5	HDI	Capro
P6	Shieldex	4,3 %	1:1.5	IPDI	DMP
P7	Shieldex	4,3 %	1:1.2	HDI	DMP
P8	Shieldex	4,3 %	1:1.2	IPDI	Capro
P9	ATP	8,6 %	1:1.5	HDI	Capro
P10	ATP	8,6 %	1:1.5	IPDI	DMP
P11	ATP	8,6 %	1:1.2	HDI	DMP
P12	ATP	8,6 %	1:1.2	IPDI	Capro
P13	ATP	4,3 %	1:1.5	HDI	Capro
P14	ATP	4,3 %	1:1.5	IPDI	DMP
P15	ATP	4,3 %	1:1.2	HDI	DMP
P16	ATP	4,3 %	1:1.2	IPDI	Capro

calculated in the following way, which is shown by an example. The interactions of (a) anticorrosive pigment content with (b) OH/ NCO ratio are a1b1, a1b2, a2b1, a2b2, where 1 corresponds to high level and 2 to low level. To calculate the interaction of a1b1, the results of a1 (5) and b1 (5) were used and then divided by 2. From the result, which is 5, it can be concluded that there is no interaction between levels of OH/ NCO ratio and 8.6 % anticorrosive pigment content, because the value remained indifferently. The same was proceeded for the other interactions of a1b2, a2b1, a2b2.

2.1.4. Preparation of free coating films

Free coating films were prepared by applying self-adhesive polytetrafluoroethylene (PTFE) films to degreased steel sheets. The model primer coatings were applied with a wire bar (RD Specialties, Inc.) and cured for 22 s at 300 °C in an air-circulating convection oven (Hofmann Wärmetechnik GmbH) to reach a PMT of 228 °C. Finally, the coating films (DFT = 17 µm) were stripped off.

2.2. Testing and characterization

2.2.1. Blister testing and visual evaluation

Blister testing was performed by exposing the samples as depicted in Fig. 1. A water bath was used as an evaporation source, where the bath temperature was held constant by a thermostat at 60° and 70 °C. Square coated samples (9 cm in side-length) were positioned on top. The temperature difference between the interior bath temperature and the outer constant room temperature of 23 °C resulted in a thermal gradient and a surface temperature of 50–55 °C on the backside of the samples. The described tests were designated as condensation test at 60 °C (KT60) and condensation test at 70 °C (KT70) according to the selected bath temperature. Coatings were checked daily for defects and the degree of blistering was evaluated visually according to ISO 4628-2. The obtained results of blister size and quantity were simplified by converting them to numerical values (Appendix A).

2.2.2. Evaluation of blisters by EIS

In addition to the visual evaluation of blisters, EIS measurements were performed at defined time intervals. The experimental setup consisted of a Zahner IM6 potentiostat (Zahner-Elektrik GmbH & Co. KG) with a 2-electrode setup. A copper electrode (5 cm in diameter) was used as reference electrode (Colt Laminate Tester from Zahner-Elektrik GmbH & Co. KG) and a coated steel sheet was used as a working electrode. A filter paper saturated with sodium hydrocarbonate puffer (pH 8.5, p.a. from Carl Roth GmbH & Co. KG) was placed as a contact between the two electrodes and the copper electrode was positioned on top of the coated steel sheet. The spectra were recorded with a perturbation voltage amplitude of 20 mV and the impedance was scanned between 100 MHz and 50 mHz. Sodium hydrocarbonate was chosen as an electrolyte to avoid any contamination of the coated surface with corrosive ions such as sulfate or chloride. The barrier properties of the coating were evaluated by plotting the impedance at 100 mHz as a function of the exposure time.

2.2.3. Microstructural characterization

Blistered areas were prepared by first sputtering with gold and then embedding them in an epoxy matrix. Afterwards conventional metallographic cross sections were made. Microstructural analysis was conducted using an optical microscope (Zeiss Axio Observer from Carl Zeiss Microscopy GmbH) and scanning electron microscopy (SEM) combined with elemental dispersive X-ray analysis (EDX, Tescan Clara from Tescan Orsay Holding) at an accelerating voltage of 15 keV.

2.2.4. Blister liquids: analytical characterization of blister liquids with ICP-MS and characterization of the osmotic activity

Blister liquids were extracted by using a micro-needle and syringe. The liquids were collected from blisters distributed across the samples

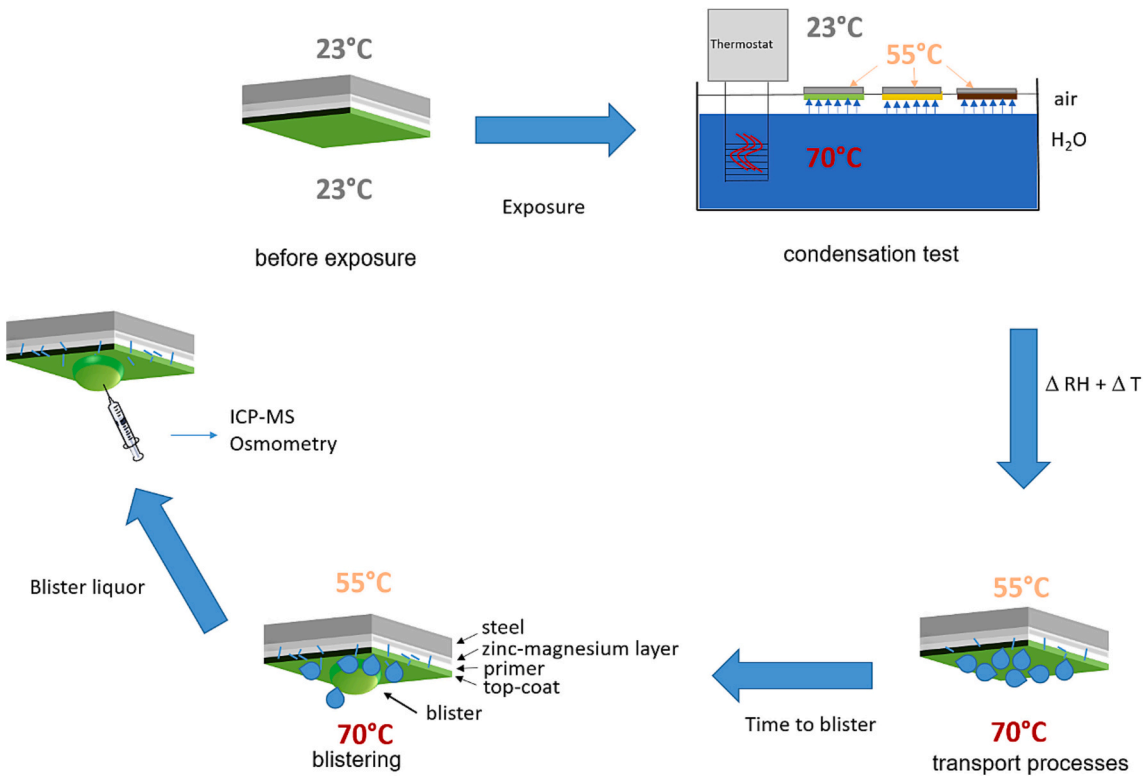

Fig. 1. Schematic representation of blister testing in this study. On top, the exposure of the coating to the condensation test is shown. Hot water vapor condenses at the samples positioned above. Due to the high temperatures, the surface temperature of the samples increases to 50 °C- 55 °C. After several weeks of exposure ("induction period"), the sample starts to blister. Then blister liquid was extracted and analyzed with ICP-MS and osmometry.

after the condensation test and total volumes of about 2–4 μL were obtained per sample (i.e., from approximately 10–20 blisters). Liquids were analyzed with Inductively Coupled Plasma - Mass Spectrometry (ICP-MS, Thermo Scientific iCAP-RQ from Thermo Fisher Scientific Inc.).

To quantify the number of osmotically active particles in the liquid, a vapor pressure osmometer, K7000 from Knauer Wissenschaftliche Geräte GmbH was used. The measurements were conducted at 40 °C, with a head temperature of 43 °C. Sodium chloride was selected as a reference standard and a calibration in the range of 1 and 100 mOsmol kg^{-1} was performed, which is below the recommended measuring range. As the blisters were destructed for each measurement, the number of measurements was limited.

2.2.5. Characterization of the leachates of free coating films

For leaching experiments, 600 mg free coating film was immersed in distilled water for 336 h at 50 °C. The conductivity of the eluates was measured and the concentrations of cations (Zn^{2+}, Ca^{2+}, Mg^{2+}, Na^{+}, Ba^{2+}, Al^{3+}) and anions (SO_4^{2-}, Cl^{-}, $H_2PO_4^{-}$) were determined by Inductively Coupled Plasma - Mass Spectrometry (ICP-MS, Thermo Scientific ICAP-RQ from Thermo Fisher Scientific Inc.), Flame Atomic Absorption Spectrometry (F-AAS; Analytic ContrAA 300 from Analytik Jena GmbH) and by anion chromatography (Thermo Science AS9-HC 4 mm Ion Pac from Thermo Fisher Scientific Inc.).

3. Results

Prior to the experiments about the effects of model primer formulations, the presence of a topcoat was found to be a precondition for the formation of blisters. Primers in combination with a PVDF-topcoat exhibited the highest sensitivity for blistering. Detailed results can be obtained in the supplementary materials (Appendix A). On primed samples without topcoat no blistering and also no signs of corrosion were observed within the usual testing period of 1000 h.

3.1. Effect of temperature gradients with increased thermal flux

The effect of temperature distribution on blistering kinetics was investigated by using a square-shaped cooling device, which was connected to a cryostat. The cooling device was positioned on top of the outer side of the panel placed above the condensation chamber. Thermal pictures of the cooled (Fig. 2 a) and uncooled (Fig. 2 d) coating show the temperature distribution. A clear dependence of the temperature distribution on blister initiation was found for the cooled coating after two weeks of exposure, as blisters formed in the uncooled areas. (Fig. 2 b). In contrast, blisters appear without a distinct pattern across the coating when no cooling device was used (Fig. 2 e). Photographs of the blisters were taken after 14 days and 21 days of exposure. Blister growth is retraced by comparing the photographs. Using a cooling device on the unexposed side, blistering starts at the hottest, outer edges and proceeds to the coolest, inner center as a function of time (Fig. 2 c). In contrast to that, blistering is random when the coating is not cooled (Fig. 2 f). From the results, it is clearly derived that blister initiation and growth is highly dependent on the temperature distribution accompanied by thermal gradients.

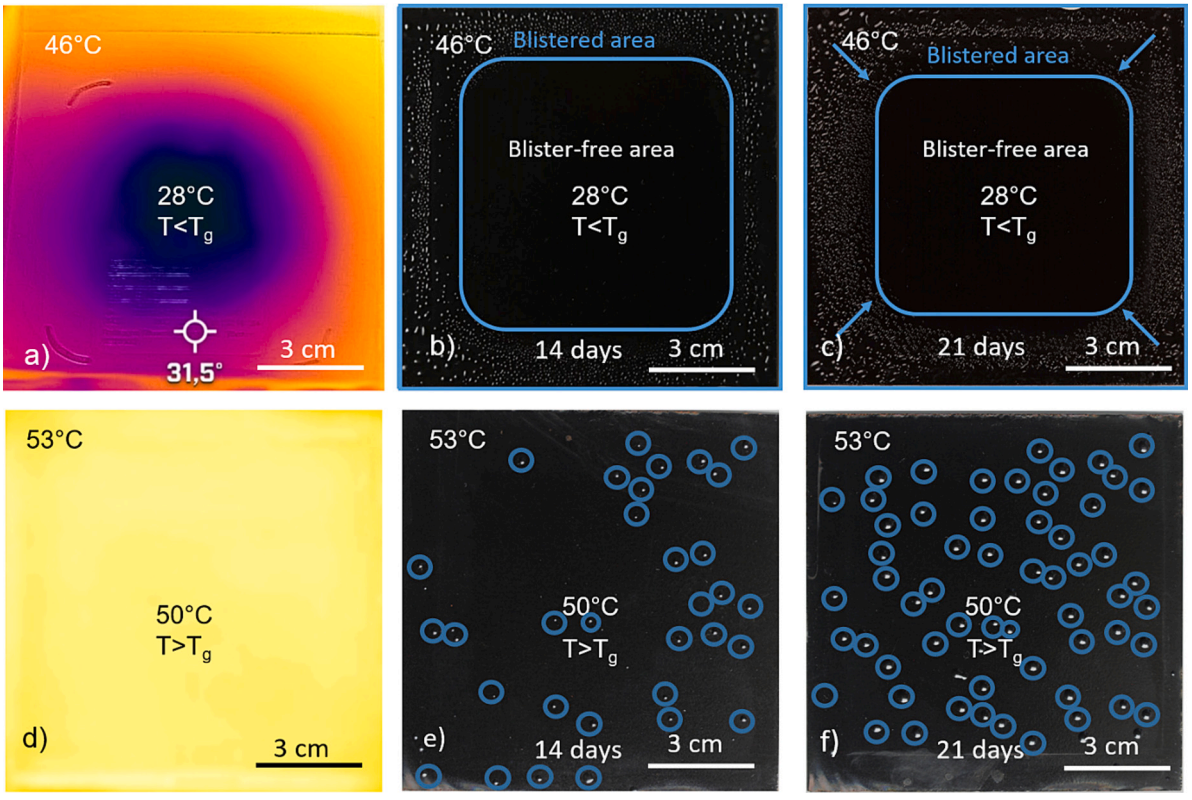

Fig. 2. By using a square-shaped cooling device, the temperature dependence of blistering was visualized. The cooling device was placed in the middle of the sample, where the coating was cooled down below the T_g of the topcoat (35 °C) as seen in the thermal picture in a). The blistered area is within the blue frames in b) and c). It is observed that blistering follows the temperature distribution in the early stages of exposure, which is shown in the photograph in b). Comparing the photographs taken after b) 14 days and c) 21 days exposure, it is noticeable that blistering proceeds in the direction from the hottest to the coldest regions as indicated with blue arrows in c). Without cooling, d-f), the surface temperature (>50 °C) is above T_g and blistering occurs without a specific pattern across the sample. The blisters in d-e) are labelled with blue circles. Blisters growth is shown after e) 14 days and f) 21 days of exposure. In contrast to the cooled coating in c), the formation of new blisters is random when the coating is not cooled (see also f). (For interpretation of the references to color in this figure legend, the reader is referred to the web version of this article.)

3.2. Systematic study of model primers

3.2.1. Evaluation techniques on blister kinetics: visual assessment vs. EIS

During the condensation tests applied in this study, blisters develop within several days and are evaluated according to ISO 4628-2. In parallel to this visual evaluation, capacity changes measured with EIS provide valuable information about the hygrothermal stability of organic coatings. However, it should be noted that the data shown here are not normalized with respect to the blistered area, but to the surface area exposed to the electrode. Fig. 3 shows the impedance ($|Z|_{100\ mHz}$) decreasing continuously with time. The impedance moduli of the higher pigmented coating (P1 + TC1) and the lower pigmented coating (P5 + TC1) were compared. $|Z|_{100\ mHz}$ is an indicator for the coating failure over time. The lower pigmented coating (P5 + TC1) shows a moderate decrease of $|Z|_{100\ mHz}$, which indicates a hygrothermal stable organic coating (Fig. 3 a). This is in accordance with visual evaluation. Blister formation resulted in a pronounced decrease of $|Z|_{100\ mHz}$ below 10^9 Ω cm^2, as shown with the higher pigmented coating (P1 + TC1) (Fig. 3 b). A direct comparison of both blister evaluation techniques indicates, that both techniques are comparable in sensitivity.

3.2.2. Influence of temperature on blister kinetics

Fig. 4 shows the KT70-blister formation kinetics for 8.6 % Shieldex (Fig. 4 a), 4.3 % Shieldex (Fig. 4 b), 8.6 % ATP (Fig. 4 c) and 4.3 % ATP (Fig. 4 d). The mean degrees of blistering were calculated from three measurements which are depicted as point-line curves. The corresponding standard deviations are displayed as shaded areas. The following conclusions can be drawn from these graphs: Primers with a low concentration of anticorrosive pigments (Fig. 4 b and Fig. 4 d) tend to exhibit a long blister induction time in contrast to primers with a high concentration of anticorrosive pigments. Therefore, the increase of the degree of blistering against the square root of the time obtains a more sigmoidal shape. In contrast, primers with a higher concentration of anticorrosive pigments exhibit a roughly linear increase.

The increase of temperature from 60 to 70 °C (Fig. 5 a, Fig. 5 b) has an accelerating effect on blister growth.

3.2.3. Individual contributions of primer components - DoE evaluation of parameters

Fig. 6 shows the influence of anticorrosive pigment content, OH/NCO ratio, trimer type and blocking agent of primers on blister kinetics. The anticorrosive pigment content (a), OH/NCO ratio (b), trimer type (c) and blocking agent (d) were tested on the tendency to KT70-blistering on HL and LL. The results of the Taguchi design of experiments are displayed in a bar chart. The length of the bar corresponds to the difference between HL and LL and indicates the impact on the degree of blistering. The content of anticorrosive pigments significantly influences blistering. The negative sign indicates a LL influence, which means that a lower anticorrosive pigment content yielded a higher resistivity towards blistering than a higher anticorrosive pigment content. All the other parameters are less significant, as they have either a minor effect on blistering or a large standard deviation.

3.3. Correlation of blistering tendency and leaching behaviour

In Fig. 7, the conductivity trend of four free films leached in distilled water is shown. Within the first 24 h, the conductivity considerably increases. After 336 h, the neutral aqueous solutions (pH 6–7) obtained total ion conductivities from 5 µS/cm to 27 µS/cm (Appendix A). Free primer films containing ATP leached in distilled water featured the highest conductivities. This is explained with a higher solubility of ATP compared to Shieldex. At the end of the test, eluates of free films were analyzed with anion chromatography, F-AAS and ICP-MS. Eluates of Shieldex - containing free primer films showed high concentrations of calcium and sodium ions, while eluates of ATP- containing free films contained high concentrations of aluminum, magnesium and orthophosphate ions (Fig. 8 and Fig. 9).

In Fig. 10, the correlation between the degree of blistering and the conductivity of the leachates is visualized. The number of dissolved ions increases with the pigmentation content applied in the coatings and subsequently, the degree of blistering increases. Conductivity measurements are thus a simple and reliable test to evaluate the tendency to blistering as the sum of ions in leachate solutions is measured.

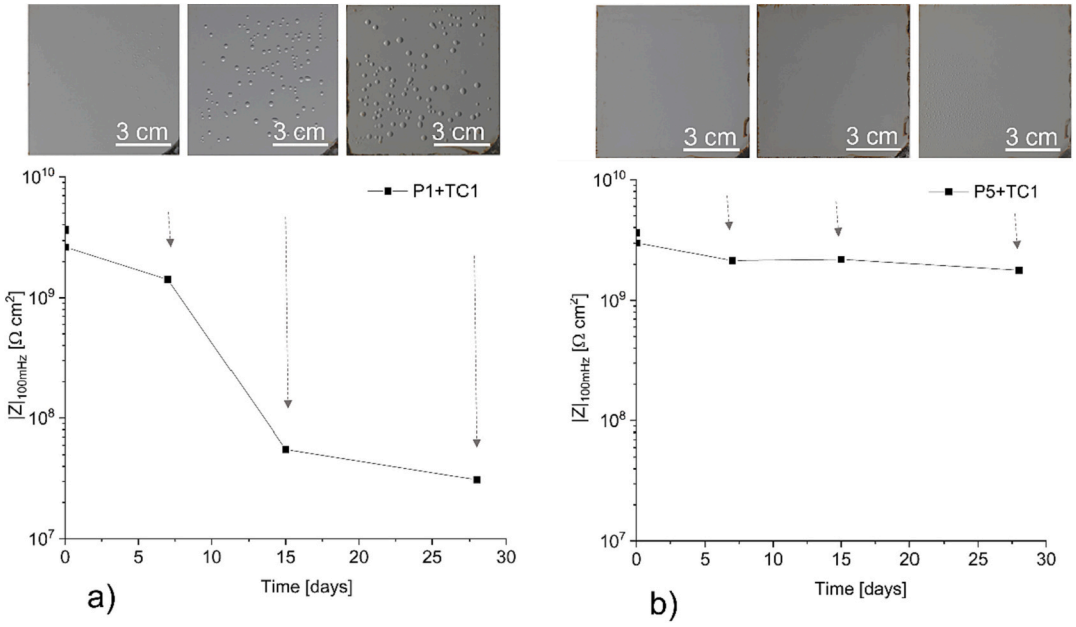

Fig. 3. Plots of the impedance |Z| at 100 mHz versus time. The higher pigmented primer (P1 + TC1) shows a significant decrease of the impedance with time (a), while the lower pigmented coating (P5 + TC1) changes only moderately (b). The changes of the impedance $|Z|_{100\ mHz}$ with time correlate with photographs from the top surface of the blistered samples.

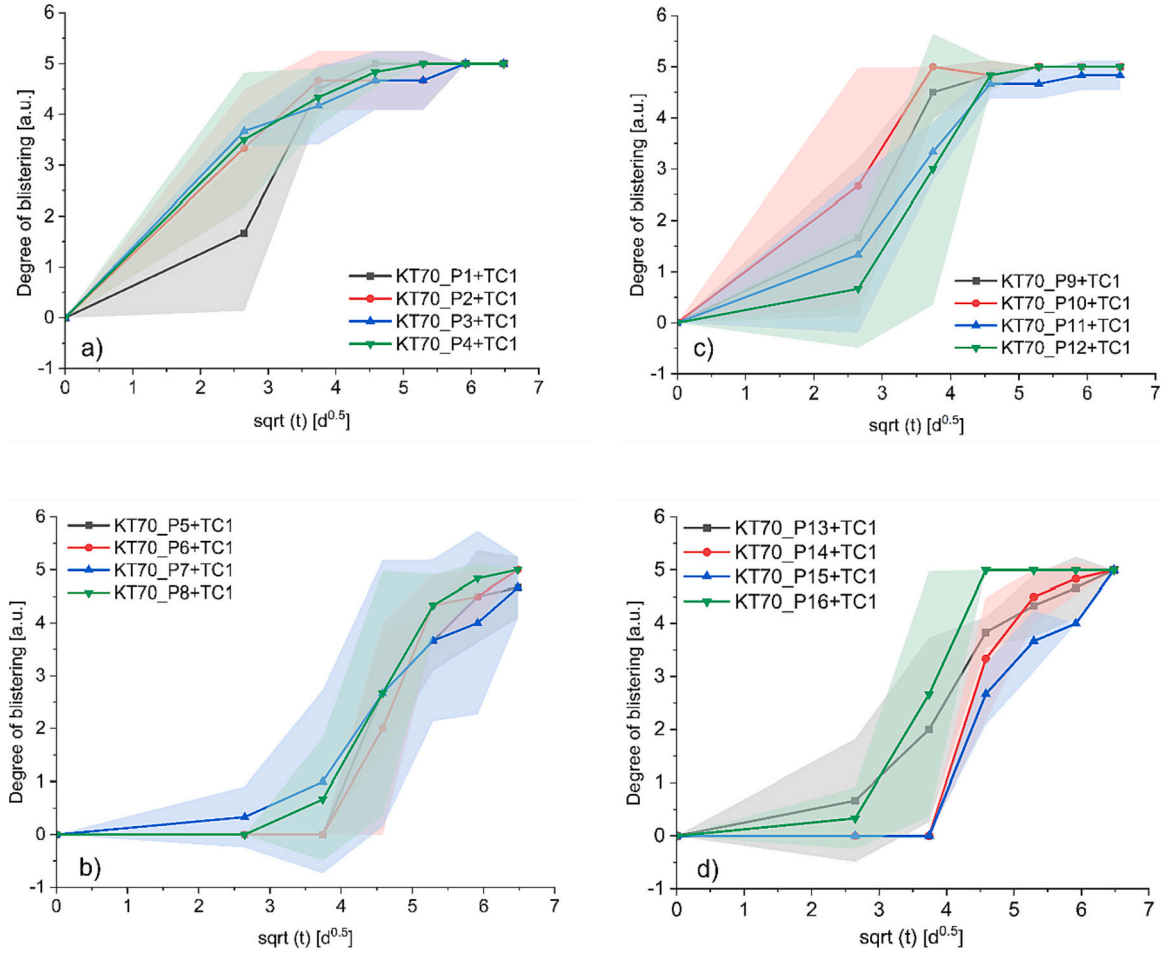

Fig. 4. Blistering kinetics of all coatings at KT70 grouped according to the anticorrosive pigment content a) 8.6 % Shieldex, b) 4.3 % Shieldex, c) 8.6 % ATP and d) 4.3 % ATP. The mean values of the degree of blistering are displayed as solid lines and the standard deviation is indicated with a shaded area.

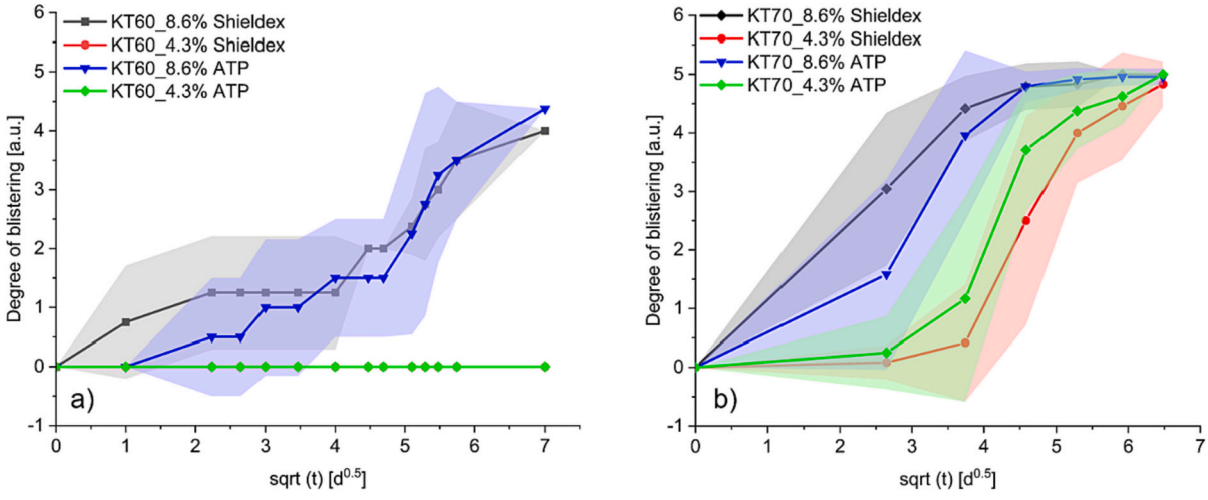

Fig. 5. Comparison of the degree of blistering versus the square-root of the time at 60 °C and 70 °C. The data in a) and b) are grouped according to the anticorrosive pigment type and content. The point-line curves depict the mean degrees of blistering from the condensation tests at 60 °C and 70 °C. The shaded area indicates the standard deviation.

3.4. Characterization of blister liquids and estimation of pressures

To characterize the liquid within the blisters, liquids were collected and analyzed by osmometry and ICP-MS.

3.4.1. Osmometry

The so-called osmolality corresponds to a sum of different anions and cations, featuring different molar masses and charges. As the prevalent species of anions and cations and the concentrations in the osmometry measurements were not specified prior to the osmometric

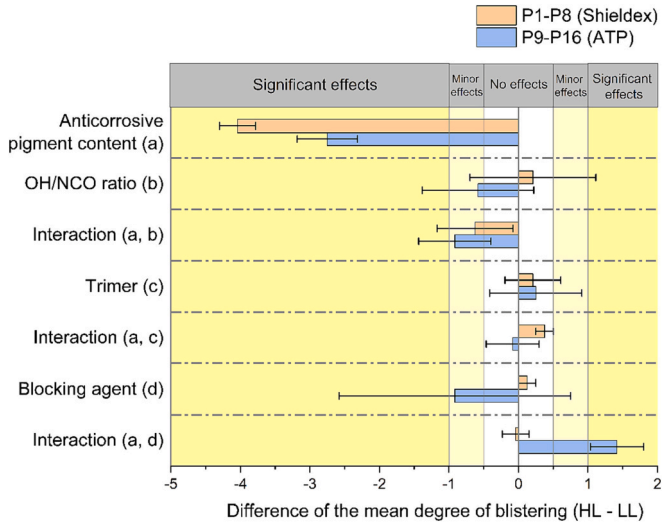

Fig. 6. Effects of coating formulation parameters on the degree of blistering. The data depicted refer to 14 days KT70 exposure, as the largest differences in the degree of blistering were observed at this stage. Three measurements were averaged, and the standard deviation was calculated. The impact of the parameters and interactions between them are demonstrated by the length of the bars and the corresponding error bars, whereby their contributions are distinguished in minor (±0,49-0,99; light yellow areas) and significant effects (> ± 0.99; bright yellow areas). Apparently, the anticorrosive pigment content has the most significant effect on blistering in Shieldex- and ATP-containing coatings. (For interpretation of the references to colour in this figure legend, the reader is referred to the web version of this article.)

measurements, the following results are referenced to sodium chloride as a calibration standard. Osmolalities ranging from 20 ± 10 to 120 ± 10 mOsmol kg^{-1} were obtained for the blister liquids (Appendix A).

3.4.2. ICP-MS

Analysis of the blister liquids reveal the localized active concentration of ions, which have not reacted to insoluble products. To prepare ICP-MS dilutions, the collected amount of blister liquid per sample (2–4 µL) were diluted in 20 mL MilliQ-water. After the measurement, the concentrations of the diluted blisters were not extrapolated to the original concentration, as the volumes of the blister liquids were too small. In general, higher ion concentrations from the coating components (calcium, magnesium, silicon, phosphorus) rather than from the metallic coating (zinc) and pretreatment of the substrate (titanium) were found. Shieldex-containing coatings featured blister liquids with calcium ions ($4*10^{-3}$–$1*10^{-2}$ mmol/L) and magnesium ions ($2*10^{-3}$–$4*10^{-3}$ mmol/L). Blister liquids with ATP contained high concentrations of magnesium ($2*10^{-2}$ -$2*10^{-1}$ mmol/L), a lower concentration for phosphorus ($5*10^{-3}$–1,3 $*10^{-2}$ mmol/L) and very low concentrations of aluminum (<$2*10^{-4}$ mmol/L). Also, ion concentrations originating from the metallic coating and the pretreatment were investigated. A mean zinc ion concentration of $1*10^{-3}$ mmol/L was found, while titanium was not detectable (<$2*10^{-5}$ mmol/L).

4. Discussion

4.1. Influence of temperature gradients within the exposed sample

The effect of temperature gradients ("cold wall effect") was assessed by cooling the unexposed side of a commercial coating with a dry film thickness of 50 µm below the glass transition temperature. In Fig. 2, it is clearly shown that osmotic blister growth depends on the temperature distribution. By cooling below the glass transition temperature, transport processes were decelerated, the water solubility and the probability of degradation were reduced. After a testing time of 49 days, no blisters were detected in the cooled areas and cross sections of the coatings were defect-free. Temperatures above the glass transition temperature (T_g) increase the network mobility of the organic coating and promote blistering. An increase of the water bath temperature from 60 °C to 70 °C e. g., accelerates osmotic blister growth of the model systems (Fig. 5).

4.2. Mechanism of blister formation in humid hot laboratory testing

The exposure to humidity and high temperature initiates several processes in the coating such as water sorption, swelling, mobilization of soluble species and finally macroscopic blistering. In the following sections, the steps prior to blistering are briefly explained.

4.2.1. Leaching of anticorrosive pigments

In the condensation test, water vapor of elevated temperature (typically 50–70 °C) condenses at the coating surface (Fig. 1). The presence of water at the interfaces of the anticorrosive pigments and partly also fillers lead to solubilization of ions [23–25]. These ions react with the metal coating and form a protective layer against corrosion at the steel surface. A detailed mechanistic understanding of leaching processes is presented in a recent work of [15,26]. Emad [15] uses the percolation theory for describing the leaching mechanisms in a coating. In the percolation theory, the coating is a 3D-network with long-range connected pigments ("percolation threshold P_c"). The ratio of P_c and the pigment volume concentration (PVC) determines the leaching velocity and the barrier properties. If the PVC is higher than the P_c, the inhibitor pigments are depleted faster, and the coating resistance falls to low values. This model can be applied in a more general way also to our systems where we found that the absolute concentration of anticorrosive pigments in the primer determines the leaching velocity and accelerates blistering with increasing pigment concentration.

4.2.2. Predominant osmotic blistering, accelerated by cold wall effect

Ions released from anticorrosive pigments in the primer (Fig. 7, Fig. 8, Fig. 9) accumulate either at the primer-metal or primer-topcoat interface. The released ions contribute to the development of an osmotic cell. The topcoat acts a semipermeable membrane and water is drawn from the exposed surface to the osmotically active clusters. Without a topcoat, the ions are washed off and no blistering is observed. In this study, the osmotic mechanism was studied in detail. By using distilled water without corrosive species in the leaching experiments, the influence of corrosive species in studying the osmotic blistering mechanism was not investigated. However, analysis of blister liquids (3.4.2.) showed that the concentrations of zinc and magnesium ions originating from the metallic coating were lower in comparison to ions originating from inhibitors. Blisters were formed between the model primer and the PVDF topcoat, and so, ions from the metallic coating were barely present in the blister liquids. In SEM-EDX measurements (Appendix A), it was shown that the zinc-magnesium layer underneath was intact. This specific behaviour can be explained with the absence of covalent bondings between the layers that has been investigated considering formulation aspects [27–29]. Besides from that, also other factors as different permeabilities [30] and a poor wet adhesion of the PVDF topcoat [2] may have contributed to the observed phenomenon.

Blister initiation has clearly its origin from an osmotic effect and an increasing content of anticorrosive pigments correlates with a reduced blister induction time (Fig. 5). Although the process leading to blister growth is multifactorial (parallel growth of blisters and initiation of new blister sites), roughly linear sections in the kinetic plots vs. square root of time (Fig. 4) indicate, that transport processes of water and ionic species play a key role as soon as blistering can be observed. Nevertheless, deducing parameters of diffusion from this plot would be a bit of a stretch. These findings are in full agreement with the fundamental work of Pommersheim [9] and Sinko [10] who showed that blister intensity (as quantified by the blister volume) increases with the concentration of the osmotic species whereas blister growth at a constant temperature

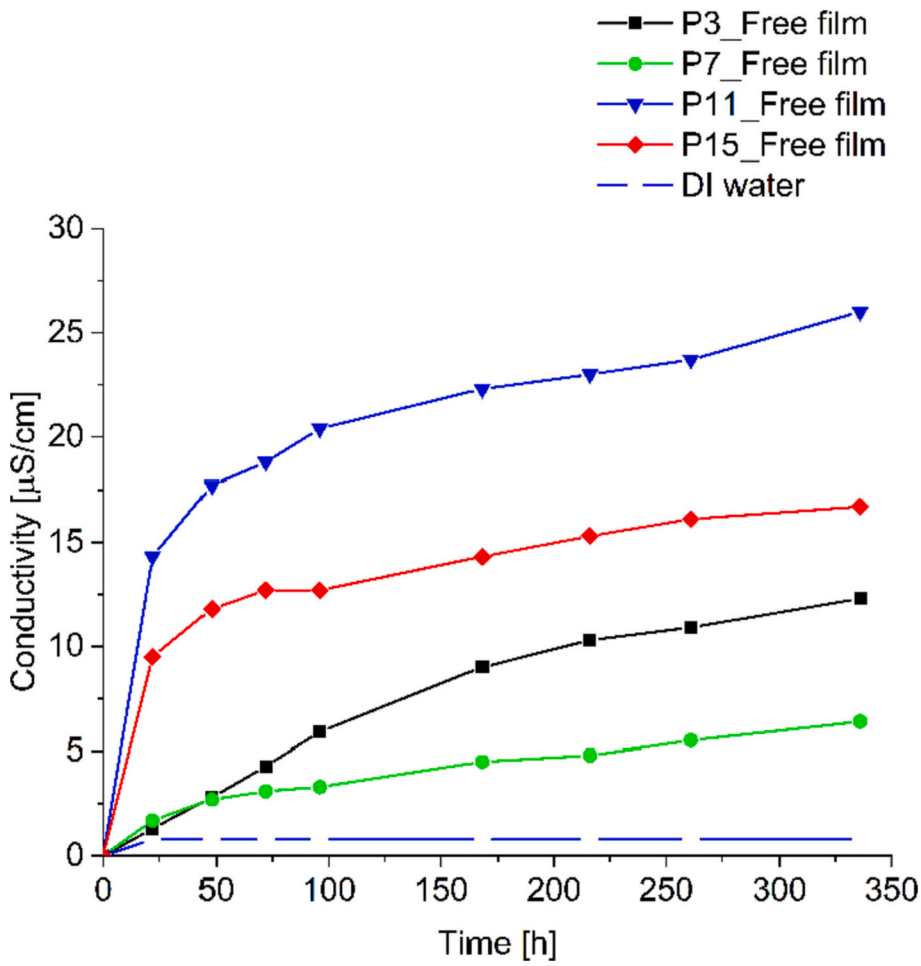

Fig. 7. Increase of the conductivity with time while leaching free films of primers in distilled water at 50 °C. The diagram shows free films of primers containing 8.6 % Shieldex (P3), 4.3 % Shieldex (P7), 8.6 % ATP (P11) and 4.3 % ATP (P15) respectively.

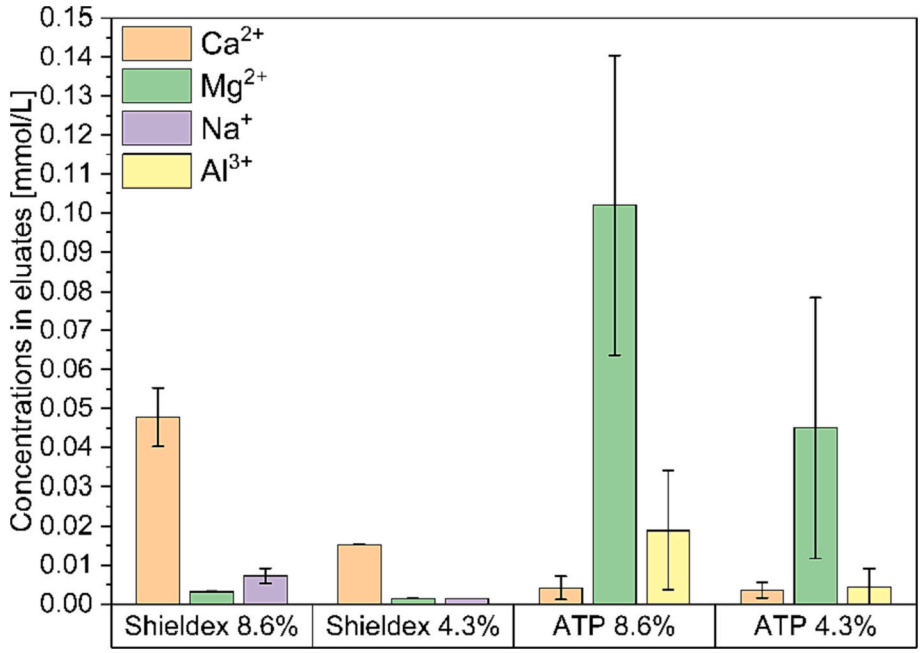

Fig. 8. The averaged concentrations of cations in leachate solutions of free primer films are shown. High concentrations of Ca^{2+} ions were found in leachates of Shieldex-containing primers, while ATP-containing primers enclosed mainly Mg^{2+} ions.

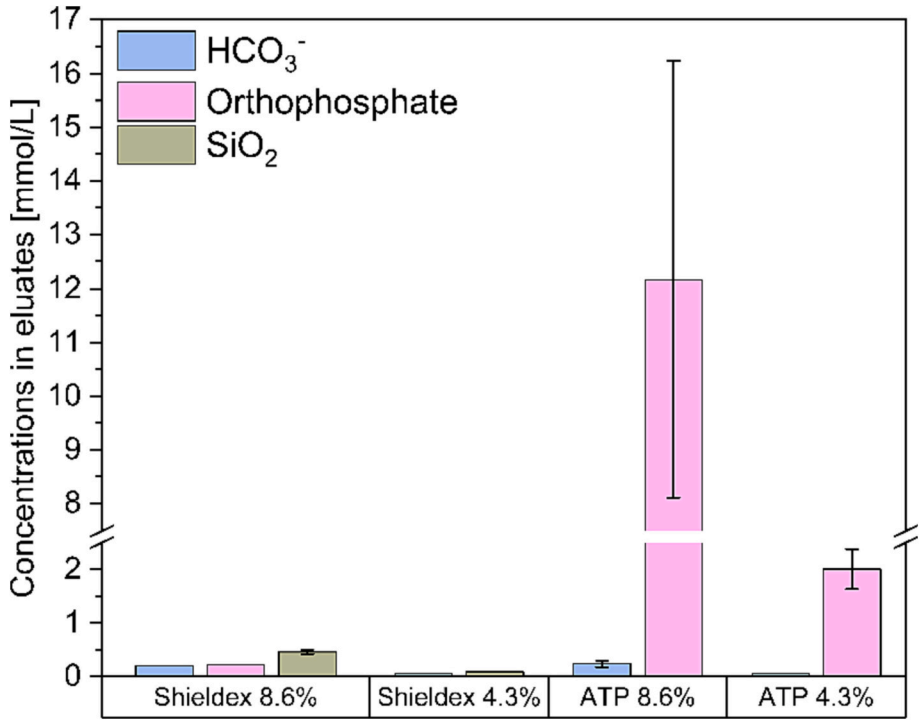

Fig. 9. The averaged concentrations of anions in leachate solutions of free primer films are shown. High concentrations of orthophosphate ions were found in leachates of ATP-containing primers.

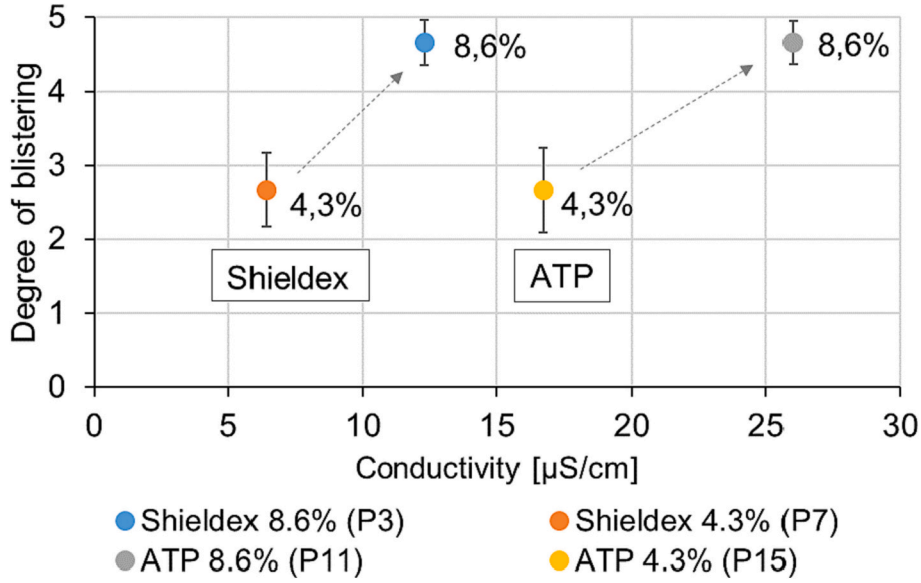

Fig. 10. Correlation between the degree of blistering after 21 days in the condensation test at 70 °C and the conductivity of the leachates in distilled water after 336 h.

follows the square root of time $t^{0,5}$ (Fickian law).

4.3. Osmotic pressure

The number of particles present in an osmotic cell (i.e., the osmolality [mOsmol kg^{-1}]) can be determined via osmometry. The osmotic pressure (π) in the accumulated blister liquid is calculated according to Eq. (1) [31],

$$\pi = c^{*}R^{*}T \quad (1)$$

where the measured osmolality (c), the ideal gas constant (R) (8,3145 kPa L mol^{-1} K^{-1}) and the temperature (T) of 313 K are used. As a result, pressures in the blisters of 0.5 bar ±0.25 bar to 2.8 bar ±0.25 bar were calculated for this work.

Van der Meer-Lerk et al. [5] published an equation (Eq. (2)) to estimate the pressure inside a blister (P_k), which is based on Timoshenko's Theory of Plates and Shells. For the calculation, a blister radius (r) of 850 µm and a film thickness (t) of 26 µm were measured. The height, which was 56 µm in the crosscut was estimated to be 100 µm in the liquid filled wet state (Appendix A). Typical E-moduli of 2,84 GPa ± 0.48 (E1 + TC1) and 2.97 GPa ± 0.02 (E8 + TC1) were obtained in

tensile tests at room temperature (Appendix A). Coil coatings in general exhibit a strong temperature dependence of the E-modulus around service temperature and in dependence of the crosslink density, values ranging from 2 MPa (rubbery state) up to 2,5 GPa (glassy state) are found [32]. Considering the testing temperature of 70 °C and fully saturation of the coating with water, it seems reasonable, that the coating film is somewhere between the rubbery and the glassy state. As an educated guess, an E-Modulus of 500 MPa was chosen for the calculations.

$$P_k = \frac{E}{0,176} * \frac{t^4}{r^4} * \left(\frac{h}{t} + 0,583 * \frac{h^3}{t^3}\right) \quad (2)$$

By adopting these values to Eq. (2), an internal liquid pressure (P_k) of 0.093 MPa was obtained. The measured values from the osmometry measurements are in the same range as the theoretically calculated pressures (0.05 ± 0.025 MPa to 0.28 ± 0.025 MPa). Other authors [33] rely on calculations including failure mechanics-based models.

4.4. Blister-evaluation: visual or via EIS

In our study, one goal was to find a method to characterize early stages of blistering. As the impedance at a low frequency displays the barrier properties of organic coatings [1,19], the impedance was measured down to 50 mHz (Fig. 3). Although impedance data are in good agreement with the visual observation of blisters, no higher sensitivity of EIS was found in respect of early stages of blistering as reported earlier [19]. This is true for both evaluation modes – the impedance at 100 mHz [34] as well as the breakpoint frequency method [35] (Appendix A). To detect signals from the metal-paint interface, a more sophisticated measurement-setup (e.g., localized EIS) would be required to increase the sensitivity of the detection.

4.5. Leaching tests: quick and reliable techniques to investigate the sensitivity to osmotic blistering

A fast and reliable method to rank the tendency towards osmotic blistering is a leaching test performed with free primer films. Conductivity measurements provide a simple and efficient method to roughly estimate the leaching rates of the embedded anticorrosive pigments (Fig. 7). Further analysis of leachate solutions show that Shieldex-containing primers elude high concentrations of magnesium, sodium, and silicon dioxide. Correspondingly, high concentrations of magnesium, aluminum and orthophosphate ions are released from ATP-containing primers (Fig. 8, Fig. 9).

In respect to the analyzed concentrations of cations, higher concentrations of hydrogen carbonate, silicon oxide and orthophosphate have been found in the leachates. A balance of charge is premised, even though the concentrations of the conjugated acid- base pairs have not been determined. Even without a comprehensive analytical characterization of all ionic species, the results presented provide a valuable tool for the estimation of the tendency to leaching and osmotic blistering.

5. Conclusion

In this study, the influence of the composition of model primer formulations on blister formation and growth in a QCT-type condensation test were investigated. The presence of a topcoat was found to be a precondition for blistering. Two-layered coatings were applied on chromate-free pretreated HDG steel, where the composition of the model primer was varied. The chosen test setup with cold wall conditions resulted in accelerated osmotic blister formation at temperatures of 60 and 70 °C. The pigment content of the primer, the topcoat chemistry and the test temperature were the key parameters influencing blistering kinetics.

Crack formation was found to start at structural weak spots of the coating, i.e., at the primer interface to the metallic coating, within the primer and at the interface between primer and the PVDF topcoat. The latter behaviour was attributed to weak adhesion between primer and PVDF topcoat.

Blister kinetics revealed two aspects: While induction time of osmotic blistering correlates to the number of osmotically active species (i.e., ionic concentration), blister growth as observed by the increase of blisters in size and number seems to be controlled by mass transport (water and ionic species) and increases with the applied temperature gradient. The surface temperature has to exceed the T_g of the coating to initiate osmotic blistering in the condensation test. Main source of the soluble ions is the anticorrosive primer pigmentation. Leaching experiments provide a simple and reliable method to predict the tendency towards osmotic blistering in condensation type testing.

Blister liquids were analyzed, and the presence of ions has been proven by ICP-MS measurements. The number of osmotically active particles was determined with osmometry and corresponding pressure values have been estimated in a reasonable range to account for the observed osmotic effect.

To sum up, the main mechanism identified for coil-coatings in humid-hot laboratory testing is osmotic blistering assisted by a cold wall temperature gradient that is active at testing temperatures above the topcoat glass transition temperature. It has been shown that the material selection of a topcoat and the solubility of anticorrosive pigments embedded in a primer are important parameters to delay osmotic blister initiation and decelerate blister growth.

CRediT authorship contribution statement

B. Obereigner: Investigation, Formal analysis, Data curation, Writing - original draft **G. Mayr:** Conceptualization, Methodology, Visualization, Discussion. **B. Strauß:** Project administration, Validation, Writing – review & editing. **P. Bognar:** Resources, Discussion. Writing – review & editing. **S. Ngo:** Experimental design, Writing – review & editing. **K. Bretterbauer:** Writing – review & editing. **C. Paulik:** Supervision, Writing - review & editing.

Declaration of competing interest

The authors declare that they have no known competing financial interests or personal relationships that could have appeared to influence the work reported in this paper.

Data availability

The raw/processed data required to reproduce these findings cannot be shared at this time as the data also forms part of an ongoing study.

Appendix A. Supplementary data

Supplementary data to this article can be found online at https://doi.org/10.1016/j.porgcoat.2022.107373.

References

[1] T. Prosek, A. Nazarov, J. Stoulil, D. Thierry, Evaluation of the tendency of coil-coated materials to blistering: field exposure, accelerated tests and electrochemical measurements, Corros. Sci. 61 (2012) 92–100, https://doi.org/10.1016/j.corsci.2012.04.026.
[2] T. Prosek, A. Nazarov, M.G. Olivier, C. Vandermiers, D. Koberg, D. Thierry, The role of stress and topcoat properties in blistering of coil-coated materials, Prog. Org. Coat. 68 (2010) 328–333, https://doi.org/10.1016/j.porgcoat.2010.03.003.
[3] M.L. Ellinger, Accelerated weathering tests, J.Oil Colour Chem.Assoc. 62 (1979) 136–141.
[4] F.E. Bedoya, Á. Bermúdez, J.G. Castaño, F. Echeverría, J.A. Calderón, Electrochemical impedance study for modeling the anticorrosive performance of coatings based on accelerated tests and outdoor exposures, J. Coat. Technol. Res. 13 (2016) 895–904, https://doi.org/10.1007/s11998-016-9803-7.

[5] L.A. van der Meer-Lerk, P.M. Heertjes, Blistering of varnish films on substrates induced by salts, J.Oil Colour Chem.Assoc. 58 (1975) 79–84.
[6] W. Funke, Blistering of paint films and filiform corrosion, Prog. Org. Coat. 9 (1981) 29–46, https://doi.org/10.1016/0033-0655(81)80014-3.
[7] M.H. Nazir, Z.A. Khan, A. Saeed, K. Stokes, A model for cathodic blister growth in coating degradation using mesomechanics approach, Mater. Corros. 67 (2016) 495–503, https://doi.org/10.1002/maco.201508562.
[8] J.R. Kosek, J.N. Dupont, A.R. Marder, Effect of porosity on resistance of epoxy coatings to cold-wall blistering, Corros. Sci. 51 (1995), https://doi.org/10.5006/1.3293563.
[9] J.M. Pommersheim, T. Nguyen, Prediction of blistering in coating systems, in: G. P. Bierwagen (Ed.), Organic Coatings for Corrosion Control, American Chemical Society, Washington, DC, 1998, pp. 137–150.
[10] J. Sinko, Challenges of chromate inhibitor pigments replacement in organic coatings, Prog. Org. Coat. 42 (2001) 267–282, https://doi.org/10.1016/S0300-9440(01)00202-8.
[11] C.H. Hare, Blistering of paint films on metal, part 1: osmotic blistering, J.Prot.Coat. Linings 15 (1998) 45–63.
[12] O. Schneider, R.G. Kelly, Localised coating failure of epoxy coated aluminium alloy 2024–T3 in 0.5M NaCl solutions: comparison of conventional electrochemical techniques and microelectrochemical methods, Corros. Sci. 38 (2007) 119–128, https://doi.org/10.1179/147842203767789195.
[13] L.A. van der Meer-Lerk, P.M. Heertjes, The influence of pressure on blister growth, J.Oil Colour Chem.Assoc. 64 (1981) 30–38.
[14] L.A. van der Meer-Lerk, P.M. Heertjes, Mathematical model of growth of blisters in varnish films on different substrates, J.Oil Colour Chem.Assoc. 62 (1979) 233–272.
[15] S.G.R. Emad, X. Zhou, S. Morsch, S.B. Lyon, Y. Liu, D. Graham, S.R. Gibbon, How pigment volume concentration (PVC) and particle connectivity affect leaching of corrosion inhibitive species from coatings, Prog. Org. Coat. 134 (2019) 360–372, https://doi.org/10.1016/j.porgcoat.2019.05.008.
[16] S.G.R. Emad, X. Zhou, S.B. Lyon, G.E. Thompson, Y. Liu, G. Smyth, D. Graham, D. Francis, S.R. Gibbon, Influence of volume concentration of active inhibitor on microstructure and leaching behaviour of a model primer, Prog. Org. Coat. 102 (2017) 71–81, https://doi.org/10.1016/j.porgcoat.2016.04.039.
[17] M. Kopeć, B.D. Rossenaar, K. van Leerdam, A.N. Davies, S.B. Lyon, P. Visser, S. R. Gibbon, Chromate ion transport in epoxy films: influence of BaSO4 particles, Prog. Org. Coat. 147 (2020), 105739, https://doi.org/10.1016/j.porgcoat.2020.105739.
[18] Y. Prawoto, Unified model for blister growth in coating degradation using weight function and diffusion concepts, Mater. Corros. 63 (2012) 9999, https://doi.org/10.1002/maco.201106404.
[19] E.D. Schachinger, R. Braidt, B. Strauß, A.W. Hassel, EIS study of blister formation on coated galvanised steel in oxidising alkaline solutions, Corros. Sci. 96 (2015) 6–13, https://doi.org/10.1016/j.corsci.2014.12.010.
[20] A. Miszczyk, K. Darowicki, Effect of environmental temperature variations on protective properties of organic coatings, Prog. Org. Coat. 46 (2003) 49–54, https://doi.org/10.1016/S0300-9440(02)00188-1.
[21] X. Shi, B.R. Hinderliter, S.G. Croll, Environmental and time dependence of moisture transportation in an epoxy coating and its significance for accelerated weathering, J. Coat. Technol. Res. 7 (2010) 419–430, https://doi.org/10.1007/s11998-009-9209-x.
[22] F. Deflorian, S. Rossi, M. Fedel, Organic coatings degradation: comparison between natural and artificial weathering, Corros. Sci. 50 (2008) 2360–2366, https://doi.org/10.1016/j.corsci.2008.06.009.
[23] J.S. Laird, P. Visser, S. Ranade, A.E. Hughes, H. Terryn, J.M.C. Mol, Li leaching from lithium carbonate-primer: an emerging perspective of transport pathway development, Prog. Org. Coat. 134 (2019) 103–118, https://doi.org/10.1016/j.porgcoat.2019.04.062.
[24] P. Visser, S. Ranade, J.S. Laird, A.M. Glenn, A.E. Hughes, H. Terryn, J.M.C. Mol, Li leaching from Li carbonate-primer: transport pathway development from the scribe edge of a primer/topcoat system, Prog. Org. Coat. 158 (2021), 106284, https://doi.org/10.1016/j.porgcoat.2021.106284.
[25] T. Prosek, D. Thierry, A model for the release of chromate from organic coatings, Prog. Org. Coat. 49 (2004) 209–217, https://doi.org/10.1016/j.porgcoat.2003.09.012.
[26] P.J. Denissen, V. Shkirskiy, P. Volovitch, S.J. Garcia, Corrosion inhibition at scribed locations in coated AA2024-T3 by cerium- and DMTD-loaded natural silica microparticles under continuous immersion and wet/dry cyclic exposure, ACS Appl. Mater. Interfaces 12 (2020) 23417–23431, https://doi.org/10.1021/acsami.0c03368.
[27] S.J. Hinder, J.F. Watts, C. Lowe, Surface and interface analysis of complex polymeric paint formulations, in: Surface and Interface Analysis, 2006, pp. 557–560, https://doi.org/10.1002/sia.2325.
[28] S.J. Hinder, C. Lowe, J.T. Maxted, J.F. Watts, Migration and segregation phenomena of a silicone additive in a multilayer organic coating, Prog. Org. Coat. 54 (2005) 104–112, https://doi.org/10.1016/j.porgcoat.2005.04.007.
[29] S.J. Hinder, C. Lowe, J.T. Maxted, C. Perruchot, J.F. Watts, Intercoat adhesion failure in a multilayer organic coating system: an X-ray photoelectron spectroscopy study, Prog. Org. Coat. 54 (2005) 20–27, https://doi.org/10.1016/j.porgcoat.2005.03.012.
[30] M. Hoseinpoor, T. Prošek, J. Mallégol, Novel approach to measure water vapor permeability in pre-painted metals using adapted cup method: correlation between permeation rate and tendency to blistering, Prog. Org. Coat. 169 (2022), 106917, https://doi.org/10.1016/j.porgcoat.2022.106917.
[31] P.W. Atkins, J. de Paula, Physikalische Chemie, 5th ed., Wiley-VCH, Weinheim, 2013.
[32] I. Giannakopoulos, A.C. Taylor, A modelling study of the visco-elastic behaviour of polyester-based coil coatings, Prog. Org. Coat. 76 (2013) 1556–1566, https://doi.org/10.1016/j.porgcoat.2013.06.010.
[33] J.C.M. Li, K.Him Lo, B.T.A. Chang, Blister initiation mechanism of FBE coatings, in: Corrosion 2019, NACE International 2019, 2019, pp. 1–11, in: http://onepetro.org/NACECORR/proceedings-pdf/CORR19/All-CORR19/NACE-2019-13508/1140058/nace-2019-13508.pdf/1.
[34] M.J. Gimeno, S. Chamorro, R. March, E. Oró, P. Pérez, J. Gracenea, J. Suay, Anticorrosive properties enhancement by means of phosphate pigments in an epoxy 2k coating.Assessment by NSS and ACET, Prog. Org. Coat. 77 (2014) 2024–2030, https://doi.org/10.1016/j.porgcoat.2014.04.004.
[35] Z. Feng, G.S. Frankel, Evaluation of coated Al alloy using the breakpoint frequency method, Electrochim. Acta 187 (2016) 605–615, https://doi.org/10.1016/j.electacta.2015.11.114.